High-frequency standing longitudinal acoustic resonances in supported thin films

X. Zhang, R. S. Bandhu, and R. Sooryakumar
Department of Physics, The Ohio State University, Columbus, OH 43210

B. T. Jonker
Naval Research Laboratory, Washington DC 20375-5343

(Received 10 April 2002; revised manuscript received 25 September 2002; published 12 February 2003)

Inelastic light scattering from epitaxial ZnSe films grown on GaAs reveal a large number of near equally spaced phonon modes with characteristic frequencies that depend on the film thickness and scale as the harmonics of a closed-end organ pipe. These periodic excitations that extend well beyond 100 GHz are identified as confined longitudinal acoustic resonances with negligible in-plane wave vector components. The calculated scattering cross sections, which consider the elasto-optic and surface/interface ripple channels in the film and substrate, account for all significant features of the Brillouin spectra. These include the conspicuous appearance of standing wave harmonics only beyond ~45 GHz and apparent absence of Brillouin peaks related to alternate harmonics.

DOI: 10.1103/PhysRevB.67.075407 PACS number(s): 68.60.Bs, 42.62.Fi, 68.90.+g, 68.35.Gy

INTRODUCTION

Standing acoustic waves with wave vectors directed perpendicular to the surface of supported monolayer thick films were studied in the last decade through elegant time-of-flight (TOF) measurements.[1] These helium atom scattering experiments revealed organ-pipe type modes with frequencies approaching a terahertz that are determined by the local film thickness and provide information on the film elastic properties on the microscopic scale. While the TOF experiments are applicable only to ultrathin, nanometer-thick films, in a recent report it was shown that Brillouin light scattering (BLS) is in fact an excellent probe to investigate these resonances in micron–submicron-thick films.[2] Although BLS has been widely used for investigating excitations with finite (larger than inverse film thickness) in-plane wave vectors, $K_{\parallel}$,[3–10] standing wave eigenmodes characterized *only* by discrete wave vectors, $K_{\perp}$, quantized normal to the surface (i.e., $K_{\parallel} \sim 0$), were reported for the first time recently.[2] Underlying this BLS experiment on silicon oxynitride films was the surface ripple mechanism that provided the dominant light scattering channel with the discrete harmonics extending to 50 GHz.

In this paper we report on standing wave resonances in ZnSe films wherein the $K_{\perp}$ excitations are observed to 120 GHz. In contrast to the earlier work, the elasto-optic mechanism dominates the scattering cross section in ZnSe leading to significant changes to the BLS profile. The present paper provides previously unexplored results detailing important aspects of the scattering intensities. This includes a complete analysis of the Brillouin scattering intensities that concomitantly considers contributions from elasto-optic (e-o) and surface/interface ripple channels in the film and substrate. These simulations, the first for standing wave modes in a thin film, provide direct insight into many unusual aspects of the spectra including replicating the conspicuous presence of standing wave harmonics only beyond ~45 GHz in the spectra from ZnSe films and their weakness below 40 GHz. The relative importance of the different light scattering channels is highlighted and accounts for the absence of alternate Brillouin peaks as expected from a simple organ-pipe model.

RESULTS

The three ZnSe samples used in our experiments were (001) single-crystalline epilayers grown by molecular-beam epitaxy on (001) GaAs substrates as described elsewhere.[11] Two of the films of thickness $d = 1.10$ μm and 1.25 μm were undoped ZnSe layers while the film with $d = 0.67$ μm contained about $x = 0.4\%$ of Fe ($Zn_{1-x}Fe_xSe$). The Brillouin spectra were excited at ambient temperature as described elsewhere.[2]

Figure 1 shows typical spectra at scattering angles of 0°, 30°, and 40° from the $d = 0.67$ μm thick ZnSe film. The peaks at 45 GHz and ~27 GHz are the bulk longitudinal (LA) and transverse (TA) acoustic mode, respectively, while the low frequency feature at 10–15 GHz is the longitudinal resonance (LR).[7–9] *R* identifies the Rayleigh wave with the weak shoulder evident between the Rayleigh and LR modes being a Sezawa mode.[6] The most interesting aspect of the data in Fig. 1 is the series of regularly spaced peaks that are most clearly observed beyond the LA mode and extend well past 100 GHz in the $d = 0.67$ μm film. These high frequency modes continue to be present for scattering angles θ up to ~70°. The spacing between the periodic peaks depend on the film thickness and are, respectively, 6.2, 3.9, and 3.3 GHz for the $d = 0.67, 1.1, 1.25$ μm ZnSe layers. In the vicinity of 80 GHz the harmonics superpose and ride upon the peak associated with the substrate LA mode. As shown in Fig. 2 similar data were obtained at $\theta = 0°$ from the other films where the arrows identify the standing wave sequence of each film recorded at a different free spectra range (FSR) to better resolve the peaks. From Figs. 1 and 2 it is clear that the standing wave harmonics are clearly observed only beyond 45 GHz in the BLS spectra and are conspicuously suppressed below that frequency.

THEORY AND DISCUSSION

The basic physics underlying the observation of standing wave modes follows from a simple physical analysis of an

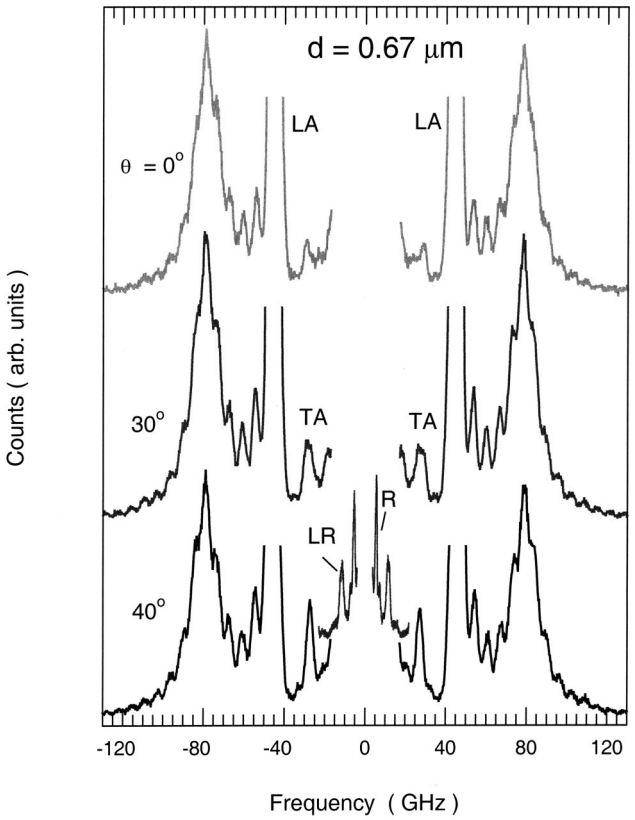

FIG. 1. Typical Brillouin spectra recorded in back-scattering from the $d=0.67\ \mu$m ZnSe sample along the [001] direction at scattering angles of $\theta=0°$, 30°, and 40°. The distinct set of periodic peaks observed beyond ~45 GHz for $\theta=0°$ are standing wave acoustic excitations. The modes labeled LA, TA, LR, and R are, respectively, the longitudinal acoustic, transverse acoustic, longitudinal resonance, and Rayleigh modes. Spectrum recorded at a lower free spectral range is also illustrated for $\theta=40°$.

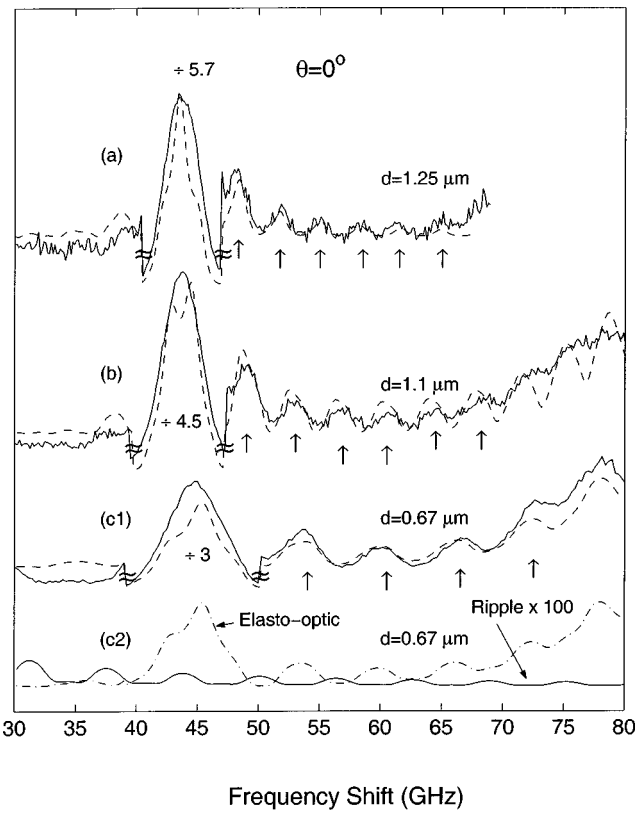

FIG. 2. BLS spectra between 45 and 90 GHz for the 0.67, 1.1, and 1.25 μm thick films recorded at a scattering angle $\theta\sim0°$. Arrows identify sequence of standing wave excitations from each film. Dashed curves are calculated total scattering cross sections. The symbol $\approx$ indicates a change of scale.

acoustic analog. The atomic vibrations at the upper and lower film surfaces, respectively, approximate an antinode and a node corresponding closely to the acoustics associated within a closed pipe. For this case the resonant standing wave mode frequencies are given by $f=(2m+1)V/4d$, where V is the speed of the waves, d the pipe length or film thickness, and m an integer. The frequency spacing δf between neighboring modes is thus given by $\delta f=0.5V/d$. While this simple intuitive model accounts for the occurrence of the multitude of near equally spaced modes, several important aspects such as the mode spacing and unusual asymmetry in the intensity profile on either side of the LA mode (~45 GHz) do not follow from this description. In order to examine the reasons for these unexpected responses, the scattering cross section that includes both volume elasto-optic and surface ripple contributions from the film and substrate and the projected local density of states (LDOS) are calculated.

For p-polarized incident light the total elasto-optic and ripple mediated light scattering cross section from a thin supported film is proportional to[12,13]

$$\frac{d^2\sigma}{d\omega d\Omega}\propto\sum_j\ |D^f_{\text{e-o}}+D^s_{\text{e-o}}+C_1u_3(k_\parallel,\omega_j,x_3=d)+C_2u_3(k_\parallel,\omega_j,x_3=0)|^2, \quad (1)$$

where index j represents the normal modes of the system. The first and second terms, respectively, represent the e-o scattering contributions from the film and substrate. The last two terms represent surface ripple contributions from the corrugated air–ZnSe interface ($x_3=d$) and ZnSe–GaAs interface ($x_3=0$), and are proportional to the phonon displacement component u_3 along the normal to the film.

The calculated total scattering cross section based on Eq. (1) is illustrated (dashed curve) in Fig. 2 in comparison to the experimental spectra. Known values for the dielectric constants,[14] elasto-optic coefficients[14,15] (K_{ij}), elastic constants (C_{ij}), and density[16,17] were utilized. As illustrated in Fig. 2 the agreement between the experimental spectra and the evaluated total cross section is good. In particular, the calculations accurately reflect the strong scattering in the vicinity of the LA peak of the film and substrate, the periodicity of standing modes and their strong (weak) cross section beyond (below) the LA frequency of ZnSe. Consistent with the relatively large elasto-optic coefficients for ZnSe films, the e-o channel dominates the scattering. As illustrated in ($c2$) of Fig. 2 for the $d=0.67$ μm film, the ripple contribution is two orders of

magnitude weaker. Further, the good fits confirm that the calculations also reveal the mode spacing (δf) to be about twice the value expected from the simple organ-pipe analog as discussed earlier.

Changes in scattering cross-section at the LA mode frequency

For the $\theta=0°$ backscattering experiments ($K_\parallel=0$), the normal modes separate into purely longitudinal or transverse excitations. Numerical simulations indicate the normal mode that predominantly determines the BLS intensity profile is dominantly longitudinal in character. Of the six partial waves within the film associated with this normal mode, only the two longitudinal components have significant amplitudes A^n ($n=1,2$) with the related amplitudes for the four transverse components (A^{3-6}) being two orders lower in magnitude. Thus the corresponding mode displacement can be written as

$$u_3^f(k_\parallel=0,x_3,\omega)=A^1\exp\{ik_3^{(1)}x_3\}+A^2\exp\{ik_3^{(2)}x_3\},$$

where

$$k_3^{1,2}=\pm\sqrt{\frac{\omega^2\rho}{c_{11}}}$$

and $\pm$ indicates mode propagation in opposite directions.

Since the e-o channel dominates scattering (Fig. 2), the total elasto-optic ($D^f_{\text{e-o}}+D^s_{\text{e-o}}$) backscattered intensities for a standing mode ($K_\parallel=0$) can be simplified as

$$\frac{d^2\sigma}{d\omega d\Omega}\propto\left|K^f_{12}(\varepsilon_s n_f+\varepsilon_f n_s)^2\left\{\frac{B^{(1)}}{2n_fk_0-k_{3f}^{(1)}}+\frac{B^{(2)}}{2n_fk_0-k_{3f}^{(2)}}\right\}+4(\varepsilon_f n_f)^2K^s_{12}\left\{\frac{k_{3s}^{(1)}A_s^1}{2n_sk_0-k_{3s}^{(1)}}+\frac{k_{3s}^{(2)}A_s^2}{2n_sk_0-k_{3s}^{(2)}}\right\}\right|^2, \tag{2}$$

where $B^{(n)}=k_{3f}^{(n)}A_f^n[\exp(ik_{3f}^{(n)}d)\exp(-i2n_fk_0d)-1]$. Scripts s and f identify substrate and film, respectively, and k_0 the photon wave vector. The BLS intensities in the range of the film LA mode (42–48 GHz) are largely controlled by the first term in Eq. (2) when total wave vector is conserved, i.e., $2n_fk_0\sim k_{3f}^{(1)}$. Similarly around the GaAs substrate LA mode ($\sim$79 GHz), the third term in Eq. (2) dominates. Away from these special frequencies all four terms in Eq. (2) generally contribute to the total intensity with the sign of each term depending on the frequency. In particular, the denominator of the first term changes sign at the ZnSe LA frequency and thus characteristically different behavior occurs in the scattered intensity centered at $\sim$45 GHz.

Figure 3 illustrates the elasto-optic contributions to the total BLS intensity from the film and substrate (ripple channel negligible at frequencies of interest) with the lower panel showing the phase difference between them. The dotted lines (beyond LA mode) at 53, 59, and 65 GHz indicate where these two contributions are in phase. At 50 and 56 GHz on the other hand they are out of phase by π, resulting in the disappearance of modes at these frequencies from the spectra. In contrast, below the LA frequency of ZnSe, the change in sign of the first term in Eq. (2) leads to the e-o contributions from film and substrate being out-of-phase (e.g., at

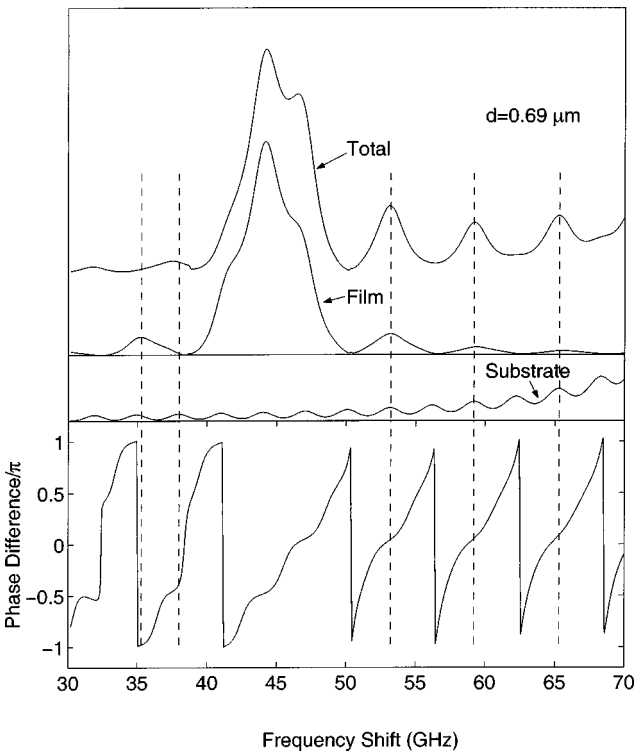

FIG. 3. Calculated Brillouin backscattering intensity at $\theta=0.1°$ for a ZnSe film of thickness $d=0.69\ \mu$m supported on a GaAs substrate. Calculations based on the elasto-optic channel that dominates the scattering. Top panel illustrates total intensity as well as contributions from the film and substrate. Lower panel shows the phase difference between e-o scattering amplitudes from film and substrate.

$\sim$35 GHz), or partially out-of phase (e.g., at $\sim$37 GHz). The ensuing interference results in the weak BLS intensities of the standing wave harmonics below 40 GHz.

We thus conclude that the observed BLS intensities are largely derived by elasto-optic coupling from both ZnSe and the substrate. The phase change of the e-o amplitudes around the LA frequency of the film results in the marked presence of standing wave harmonics only beyond $\sim$45 GHz and their weakness below 40 GHz. On the other hand, spectra from silicon oxynitride films also on GaAs were found[2] to be strong only below the film LA frequency with no discernible harmonics observed beyond it. This contrasting response is traced to the weaker e-o coefficients and dominance of surface corrugation mediated scattering in silicon oxynitride. Moreover, the e-o contribution from the substrate is also weaker for silicon oxynitride on GaAs due to the smaller magnitude of the incident photon field reaching the substrate. Thus the relative effectiveness of the two scattering channels associated with (1) surface corrugations and (2) dielectric fluctuations induced by the standing waves, account for the very different BLS response observed from the GaAs supported ZnSe and silicon oxynitride films.

Suppression of scattering intensities from alternate standing modes

In Fig. 3, a special case ($d=0.69\ \mu$m) is depicted where the ZnSe elasto-optic channel shows an almost complete

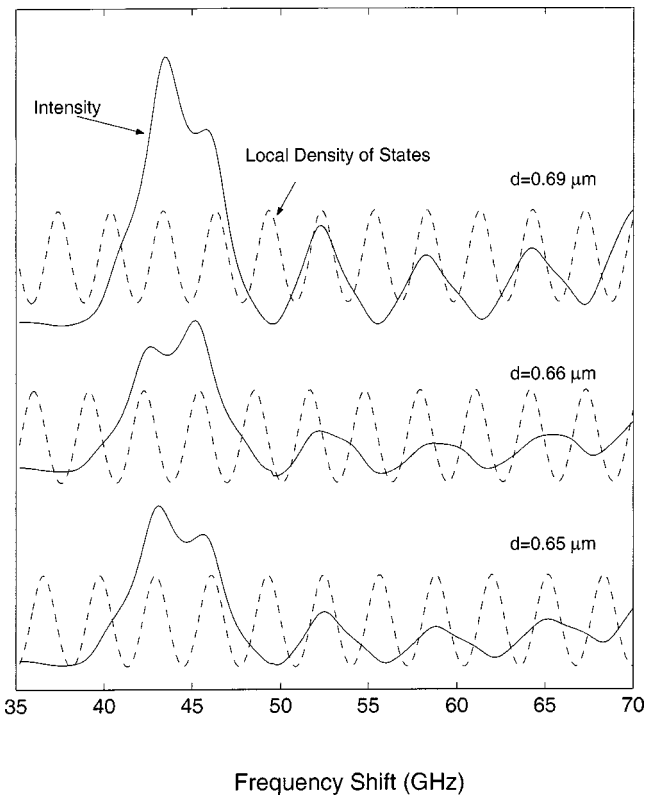

FIG. 4. Dashed curves show variation of the local mode densities D_3 calculated as a function of frequency for various film thicknesses around $d=0.67$ μm at $\theta=0.1°$. Solid curves represent calculated total Brillouin scattering cross sections.

suppression of alternate standing harmonics. This is evident in more detail in Fig. 4, where the calculated LDOS, D_3, at the free film surface ($x_3=d$) for a scattering angle of $\theta=0.1°$ is displayed (dashed curves) in comparison to the total e-o scattering intensities (solid curves) for several film thickness. The LDOS is calculated according to previous approaches[2,6] such as those given by Eq. (A18) in Ref. 6. Estimates of D_3 reveal a series of equally spaced peaks representing excitations in the film that have only $K_\perp$ wave vector components ($K_\parallel=0$), with the frequency spacing being in a good agreement with estimates deduced from the simple organ pipe analogy.

From Eq. (2) it follows that the scattering amplitude from the film is proportional to

$$D^f_{\text{e-o}} \propto [\exp(ik_{3f}^{(1,2)}d)\exp(-i2n_f k_0 d)-1]. \qquad (3)$$

Generally for odd order standing modes $\exp(ik_{3f}^{(n)}d)$ is negative while it is positive for even order.[15,18,19] Hence, depending on the sign of the phase factor $\exp(-i2n_f k_0 d)$, suppression of alternate modes can occur. From Fig. 4 it is observed that for thickness $d=0.65$ μm, the two contributing terms in Eq. (3) at ~56, 62, 68 GHz, where the LDOS are in fact maximum, destructively interfere leading to suppression of the BLS peaks. As d increases (for instance, $d=0.66$ in Fig. 4 and $d=0.67$ μm in Fig. 2), minima in the BLS intensity still occur, although they do not necessarily coincide with extrema in the local density of states. While the calculated BLS peak lineshape defined by the neighboring minima provides information about the proximity of peaks in the LDOS, the experimental resolution was inadequate to resolve their separate contributions. As a consequence, the two neighboring peaks will be evident as a single broadened BLS peak that once again effectively leads to the extinction of alternate modes. When d increases further to 0.69 μm as in Fig. 4, the analysis analogous to the case discussed above ($d=0.65$ μm) recurs and the behavior repeats periodically with thickness. We note that while the e-o contribution from the GaAs substrate is not negligible, contributions from alternate substrate modes are out-of-phase with those from the film (Fig. 3). Thus the total BLS intensities from the entire structure (film+substrate) reveal only alternate standing harmonics with the peak spacing being twice that predicted by the relation $\delta f=0.5V/d$ or the calculated LDOS (Fig. 4).

SUMMARY

In conclusion, an extended series of high frequency longitudinal standing acoustic excitations, similar to the harmonics in an organ pipe have been observed in ZnSe thin films through Brillouin scattering. The light scattering cross sections were considered in detail taking into account the ripple and elasto-optic channels in the film and substrate. We show that the strong e-o channel in ZnSe and interference between film and substrate contributions to the scattering amplitude lead to the observed BLS asymmetry below and above the film LA frequency. Moreover, in agreement with experiments, the suppression of Brillouin intensities of alternate standing wave harmonics is accounted for in the calculations.

ACKNOWLEDGMENT

Research at The Ohio State University was supported by the Army Research Office under Grant No. DAAD 19-00-1-0396, the NSF under Grant No. DMR 0205521, and at NRL by the Office of Naval Research.

[1] G. Benedek, J. Ellis, A. Reichmuth, P. Ruggerone, H. Schief, and J. P. Toennies, Phys. Rev. Lett. **69**, 2951 (1992); E. Hulpke, J. Lower, and A. Reichmuth, Phys. Rev. B **53**, 13901 (1996); D. Fuhrmann, E. Hulpke, and W. Steinhogl, Phys. Rev. B **57**, 4798 (1998).

[2] X. Zhang, R. Sooryakumar, A. G. Every, and M. H. Manghnani, Phys. Rev. B **64**, R081402 (2001).

[3] D. L. Mills and K. R. Subbaswamy, in *Progress in Optics* **XIX**, edited by E. Wolee (North-Holland, Amsterdam, 1981), p. 47.

[4] F. Nizzoli and J. R. Sandercock, in *Dynamical Properties of Sol-*

ids, edited by G. K. Horton and A. A. Maradudin (North-Holland, Amsterdan, 1990), p. 281.

[5] J. D. Comins, in *Handbook of Elastic Properties of Solids, Liquids and Gases, Dynamic Methods for Measuring the Elastic Properties of Solids*, edited by A. G. Every and W. Saches (Academic, New York, 2001), Vol. 1, p. 349.

[6] X. Zhang, J. D. Comins, A. G. Every, P. R. Stoddart, W. Pang, and T. E. Derry, Phys. Rev. B **58**, 13677 (1998).

[7] B. Hillebrands, S. Lee, G. I. Stegeman, H. Cheng, and J. E. Potts, Phys. Rev. Lett. **60**, 832 (1988).

[8] M. Chirita, R. Sooryakumar, H. Xia, O. R. Monteiro, and I. G. Brown, Phys. Rev. B **60**, R5153 (1999).

[9] X. Zhang, M. H. Manghnani, and A. G. Every, Phys. Rev. B **62**, R2271 (2000).

[10] M. Grimsditch, R. Bhadra, and I. K. Schuller, Phys. Rev. Lett. **58**, 1216 (1987).

[11] W. Y. Yu, S. Stoltz, A. Petrou, J. Warnock, and B. T. Jonker, Phys. Rev. B **56**, 6862 (1997).

[12] A. M. Marvin, V. Bortolani, and F. Nizzoli, J. Phys. C **13**, 299 (1980).

[13] V. Bortolani, F. Nizzoli, G. Santoro and J. R. Sandercock, Phys. Rev. B **25**, 3442 (1982).

[14] Dielectric constants $\varepsilon(\mathrm{ZnSe}) = 7.4 + 0.09i$ and $\varepsilon(\mathrm{GaAs}) = 17.8 + 3.21$, and elasto-optic constants of ZnSe $K_{11} = 10.47$, $K_{12} = 4.005$, $K_{44} = 3.82$ are obtained from L. Bornstein, *Numerical Data and Functional Relationship in Science and Technology*, New Series 3, Vol. 17, edited by O. Madelung (Springer-Verlag, Berlin, 1982); New Series 3, Vol. 18, edited by K.-H. Hellewege, A. M. Hellewege (Springer-Verlag, Berlin, 1984).

[15] F. Nizzoli, R. Bhadra, O. F. de Lima, M. B. Brodsky, and M. Grimsditch, Phys. Rev. B **37**, 1007 (1988).

[16] In the calculation, the elastic constants ($C_{11} = 87.8$ GPa, $C_{12} = 47.7$ GPa and $C_{44} = 38.8$ GPa) for ZnSe are obtained directly from the bulk LA and TA backscattered peaks and the LR mode along the [100] and [110] directions.

[17] The density of ZnSe (5.26 g/cm^3) and the well-known elastic constants and density for the GaAs substrate were obtained from G. W. Farnell, in *Physical Acoustics*, Volume 6, edited by W. P. Mason and R. W. Thurston (Academic, New York, 1971), p. 109.

[18] V. Bortolani, A. M. Marvin, F. Nizzoli, and G. Santoro, J. Phys. C **13**, 1607 (1980).

[19] J. M. Karanikas, R. Sooryakumar, and J. M. Phillips, Phys. Rev. B **39**, 1388 (1989).